Depth-dependent eigenenergies and damping of excitonic polaritons near a semiconductor surface

J. Lagois
Max-Planck-Institut für Festkörperforschung, Heisenbergstrasse 1, D-7000 Stuttgart 80, Federal Republic of Germany
(Received 18 December 1980)

This paper reports the experimentally observed change of exciton-polariton eigenenergies near the surface of a semiconductor. Normal-incidence-reflection spectra and attenuated-total-reflection (ATR) spectra are measured in the $n=1$ exciton-polariton energy region. It is shown that ATR spectra probe regions near the surface whereas reflection spectra probe more deeply into the crystal bulk. Model calculations, which include spatial dispersion and depth-dependent eigenenergies and damping of excitonic polaritons, yield excellent agreement with experiments for various semiconductors. This agreement proves that reflection spectra are determined not only by bulk properties of excitonic polaritons, but reveal also the properties of the transition region at the crystal surface. Therefore, information extracted so far from reflection spectra about additional boundary conditions of excitons and exciton-free surface layers may have to be revised.

I. INTRODUCTION

The electrodynamics of excitonic polaritons in semiconductors has been the subject of extensive studies in recent years. These studies investigated the basic physical properties of excitonic polaritons, which are mixed exciton-photon states corresponding to a dielectric polarization in the macroscopic description of dielectrics.[1]

Various phenomenological theories have been proposed to describe the properties of excitonic polaritons associated with spatial dispersion, i.e., the wave-vector dependence of the dielectric function of excitons.[2–4] These theories include the introduction of additional boundary conditions besides those specified by Maxwell's equations. Experimentally, reflectance,[2,5–8] transmittance,[9] and Brillouin scattering[10] yielded a great deal of knowledge about the properties of excitonic polaritons in semiconductors, and the knowledge was advanced by the experimental observation of excitonic surface polaritons.[11–14]

Most of the experiments on excitonic bulk polaritons done so far involve necessarily the crystal surface. Therefore, a comprehensive evaluation of experimental data has to include the crystal surface and its influence on the excitonic polaritons in near-surface bulk regions. Hopfield and Thomas assumed an exciton-free surface layer caused by a repulsive potential seen by the exciton.[2] This potential essentially keeps the exciton away from the surface. A more comprehensive description of excitonic polaritons approaching the surface has to include also the influence of this potential on the eigenenergies of an exciton. Some authors have already incorporated this fundamental property into their theoretical treatment.[15–22] However, a conclusive description of an exciton approaching the surface is still open to question because of lacking distinct experimental information about the modification of excitonic bulk eigenenergies near a semiconductor surface.

This paper reports the experimental observation of exciton-polariton bulk eigenenergies near the crystal surface which *deviate* from those deep in the crystal bulk. Normal-incidence-reflection and attenuated-total-reflection (ATR) spectra are measured on ZnO crystals. The experimental details are given in Sec. II. A comparison is carried out on excitonic eigenenergies obtained from fitting the experimental spectra measured on the same sample in both arrangements (Sec. III). It is shown in Sec. IV that the structure of the reflection spectra is determined mainly by crystal bulk properties, whereas the ATR spectra are determined primarily by properties of crystal regions close to the surface. The data obtained from the fits to the experimental spectra therefore lead to the result that the excitonic eigenenergies depend on the exciton's distance from the crystal surface (Sec. V). Calculations including depth-dependent eigenenergies of excitons for different semiconducting materials (Sec. VI) lead to excellent fits to experimental results and show that reflection spectra always reveal a great deal of surface properties. In Sec. VII conclusions are drawn about the reliability of properties of excitonic polaritons as previously derived from fits to reflection spectra.

II. EXPERIMENTAL

The ZnO single crystals used in the experiments are not intentionally doped, have a size of about 4×5 mm^2, and are prepared from vapor-grown material[23]

by standard lapping and etching techniques.[24] The crystal $\vec{c}$ axis lies in the reflecting plane.

The CdS crystals are as-grown platelets of about 4×8 mm^2 grown from the vapor phase. The crystal $\vec{c}$ axis lies in the reflecting plane.

The GaAs samples are layers of about 3×5 mm^2 with (100) surfaces grown by liquid phase epitaxy on semi-insulating substrates.[25] They exhibit n-type conductivity. The samples are etched in hydrochloric acid.

The crystals of ZnSe are grown by vapor transport and are not intentionally doped. The (110) surfaces have a size of about 2×4 mm^2.

The samples are held in cold helium gas (about 4 K) during the measurement. White light from a tungsten-iodine lamp is directed onto the samples with a beam divergence of about 0.3°. The reflected light passes through a linear polarizer (if indicated). The spectra are recorded using a 1-m grating spectrometer and a cooled photomultiplier with lock-in technique and digital data acquisition. The wavelength resolution is about 0.04 nm for ZnO, CdS, and ZnSe, and about 0.015 nm for GaAs.

The factor used for the conversion from vacuum wavelength to energy is 1239.8520 eV nm (Ref. 26). Additionally, the refractive index of air is included.[27]

The excitonic surface-polariton spectra are taken with an ATR arrangement.[28] A layer of aluminum about 100 nm thick is evaporated as spacing material onto the prism base surface. A cross-shaped area is held aluminum free to form the gap (refractive index $n_{\text{gap}} = 1$, gap thickness d_{gap}) between prism and sample. In this area excitonic surface polaritons are excited in the samples which are pressed against the prism of Herasil glass (refractive index $n_p = 1.475$). The internal angle of incidence is 50°. All reflectivity values refer to the prism base surface. The absolute values are obtained from the known refractive index of the crystals at energies well below the excitonic eigenenergies.

III. COMPARISON OF NORMAL-INCIDENCE REFLECTION AND ATTENUATED-TOTAL-REFLECTION IN ZnO

The inset of Fig. 1 shows the experimental arrangement for normal-incidence reflectance (angle of incidence $\alpha = 0$). The electric field $\vec{E}$ of the incoming light is polarized perpendicularly to the hexagonal $\vec{c}$ axis. In this geometry, the light excites the excitons belonging to the upper two valence bands in ZnO (A and B excitons).

The weak line in Fig. 1 exhibits an experimental normal-incidence-reflection spectrum of the $A_{n=1}$ and $B_{n=1}$ exciton polaritons in ZnO (n: main quantum number of a hydrogenlike exciton model).

The experimental spectrum is compared with a

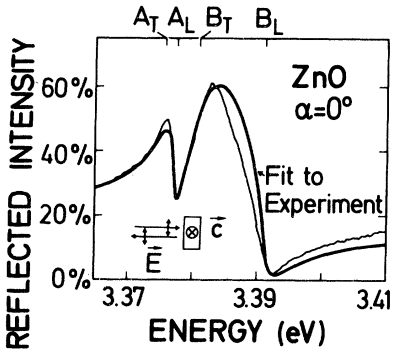

FIG. 1. Normal-incidence-reflection spectra of the $A_{n=1}$ and $B_{n=1}$ excitonic polaritons in ZnO. The inset shows the experimental arrangement. Experiment (weak line) and theory with constant exciton energy (strong line). Upper scale gives the transverse and longitudinal eigenenergies.

theoretical one (strong line) obtained from a best fit to the experiment. The optical properties of the crystal are calculated for given wave vector k and frequency ω using the dielectric function $\epsilon(\omega,k)$ of two excitonic transitions A and B showing spatial dispersion[7]

$$\epsilon(\omega,k) = \epsilon_\infty \left(1 + \frac{\omega_{BL}^2 - \omega_{AT}^2}{\omega_{BT}^2 - \omega_{AT}^2} \frac{\omega_{AL}^2 - \omega_{AT}^2}{\omega_{AT}^2 - \omega^2 + \beta_A k^2 - i\omega\Gamma_A} + \frac{\omega_{AL}^2 - \omega_{BT}^2}{\omega_{AT}^2 - \omega_{BT}^2} \frac{\omega_{BL}^2 - \omega_{BT}^2}{\omega_{BT}^2 - \omega^2 + \beta_B k^2 - i\omega\Gamma_B} \right) \tag{1}$$

with ϵ_∞ being a frequency- and wave-vector-independent background dielectric constant ($\epsilon = \epsilon_\infty$ for $\omega \to \infty$), ω_T and ω_L the transverse and longitudinal resonance frequencies at $k = 0$, and Γ the empirical damping constant ($i = \sqrt{-1}$). The influence of spatial dispersion is described by

$$\beta k^2 = (\hbar\omega_T / M) k^2 \ , \tag{2}$$

where M is the effective exciton mass and $\hbar$ is Planck's constant divided by 2π. The indices A and B denote the parameters belonging to the A and the B exciton. The reflectivity is calculated using an exciton-free surface layer of thickness d_0 (Ref. 7). The vanishing of the excitonic contribution to the macroscopic polarization at the surface is chosen as additional boundary condition.[3] The excitation of the longitudinal polariton branch is included.[7]

The damping constant Γ and the thickness d_0 of the exciton-free surface layer are chosen to be equal for the A and the B excitons (and later on for the C excitons) during all fitting procedures.

The parameters obtained from the fit are listed in Table I. The difference between the experimental and

TABLE I. Parameters of excitons in various semiconductors obtained from fits to reflection and ATR spectra with different models. (1) Constant eigenenergies and damping. (2) Depth-dependent eigenenergies and damping. (3) Parameters obtained from literature. (For explanation of the parameters see text.)

	ZnO ($A_{n=1}$)		ZnO ($B_{n=1}$)		ZnO ($C_{n=1}$)	CdS	ZnSe	GaAs
	Refl.	ATR	Refl.	ATR	Refl.	Refl.	Refl.	Refl.
(1) $\hbar\omega_T$ (eV)	3.3758	3.3760	3.3810	3.3818	3.4198	2.5517	2.8016	1.51490
$\hbar\omega_L$ (eV)	3.3776	3.3780	3.3912	3.3922	3.4317	2.5538	2.8036	1.51515
$\hbar\Gamma$ (meV)	0.7	2	0.7	2	0.7	0.15	0.4	0.02
d_0 (nm)	4	4	4	4	4	7.5	13	42
d_{gap} (nm)	. . .	80	. . .	80	. . .	. . .	. . .	. . .
(2) d_{gap} (nm)	. . .	73	. . .	73	. . .	. . .	. . .	. . .
$\hbar\omega_{TV}$ (eV)	3.3765		3.3830		3.4225	2.5518	2.8015	1.51482
$\hbar\omega_{LV}$ (eV)	3.3780		3.3927		3.4335	2.5539	2.8035	1.51515
$\hbar\Gamma_V$ (meV)	1.5		1.5		1.5	0.3	0.4	0.03
$\hbar\Delta\omega_1$ (meV)	0.8		4.0		4.0	0.60	0.15	0.03
$\hbar\Delta\omega_2$ (meV)	−0.2		−1.0		−1.0	−0.25	0.10	−0.09
$\hbar\Delta\omega_3$ (meV)	−0.15		−0.7		−0.7	−0.07	−0.05	−0.05
$\hbar\Delta\Gamma$ (meV)	0.5		0.5		0.5	0.1	0.3	0.01
d_0 (nm)	4		4		4	7.5	12.5	20
d (nm)	6		6		6	6	35	30
(3) M (m_{e0})	0.87[a]		0.87[a]		0.83[a]	0.94[b]	0.92[c]	0.298[d]
ϵ_∞	6.2[e]		6.2[e]		6.2[e]	8.0[b]	8.1[c]	12.6[d]

[a] K. Hümmer, Phys. Status Solidi (B) 56, 249 (1973).
[b] J. Voigt, M. Senoner, and I. Rückmann, Phys. Status Solidi (B) 75, 213 (1976).
[c] G. E. Hite, D. T. F. Marplé, M. Aven, and B. Segall, Phys. Rev. 156, 850 (1967).
[d] D. D. Sell, S. E. Stokowski, R. Dingle, and J. V. DiLorenzo, Phys. Rev. B 7, 4568 (1973).
[e] B. Segall, Phys. Rev. 163, 769 (1967)

theoretical spectra in Fig. 1 at energies around B_L (longitudinal B exciton energy) is known to appear for ZnO,[6] but has not yet been explained. An interpretation follows from the results in Sec. V.

The excitonic surface-polariton spectra are taken with an ATR arrangement as shown in the inset of Fig. 2. Light linearly polarized parallel to the plane of incidence is totally reflected inside the prism. An evanescent wave propagating along the prism base excites an excitonic surface polariton associated with the A and B excitons in ZnO. The wave vector $k_{\parallel}$ parallel to the crystal surface is given by

$$k_{\parallel} = n_p \sin\alpha k_{vac} \tag{3}$$

(α is the angle of incidence on the prism base surface; k_{vac} is the wave vector in vacuum). The excitation in the crystal leads to an outcoupling of intensity from the totally reflected light. This outcoupling is observed as a decrease of the internally reflected intensity in the ATR spectrum.

The upper part of Fig. 2 shows an experimental ATR spectrum (weak line) taken on the same samples as the reflection spectrum of Fig. 1. The experimental ATR spectrum is fitted with a theoretical one (strong line) of the $A_{n=1}$ and $B_{n=1}$ excitonic surface polaritons in ZnO using the dielectric function $\epsilon(\omega,k)$ of Eq. (1).[29] The parameters obtained from the best ATR fit are also listed in Table I.

It should be pointed out that the properties of excitonic surface polaritons, and thus of the ATR spectra, are determined by the refractive index of the adjacent medium and by $\epsilon(\omega,k)$, the bulk excitation's dielectric function which determines also the reflection spectra.[13] Therefore, the parameters in Table I obtained from fits to ATR spectra are, in the model used so far, the parameters of the bulk dielectric function $\epsilon(\omega,k)$ of Eq. (1).

The comparison of the parameters obtained from fits to reflection and to ATR spectra shows two striking results. First, the empirical damping constant Γ used in the dielectric function differs by a factor of about 3. Second, the excitonic eigenenergies obtained by fitting ATR spectra are considerably higher than those obtained by fitting reflection spectra, although both theoretical spectra are determined by the same dielectric function containing the excitonic eigenenergies of the crystal bulk. This deviation amounts to about 10% of the splitting between the transverse and the longitudinal eigenenergies and is conspicuous in the lower part of Fig. 2 where the

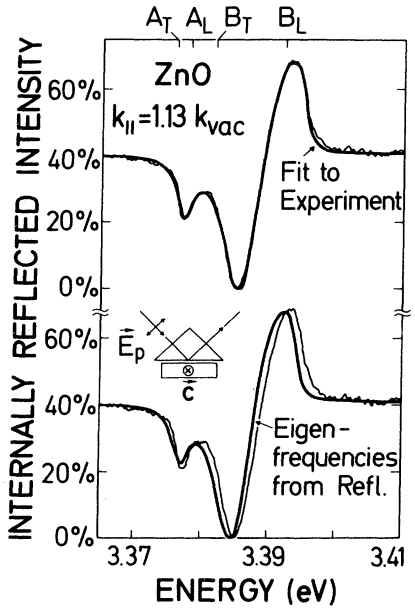

FIG. 2. Attenuated-total-reflection spectra of the $A_{n=1}$ and $B_{n=1}$ excitonic polaritons in ZnO. The wave vector $k_{||}$ of the excitonic surface polariton is given by the angle of incidence and the prism's refractive index. Upper part: Experiment (weak line) and theory with constant exciton energy (strong line) calculated with parameters obtained from fit to the experimental ATR spectrum. Upper scale gives the transverse and longitudinal eigenenergies. Lower part: Theory with constant eigenenergies obtained from fit ot the experimental *reflection* spectrum.

ATR spectrum is calculated with the eigenenergies obtained from the reflection fit. The theoretical spectrum (strong line) is compared with the same experimental spectrum (weak line) as in the upper part of Fig. 2.

The results for the eigenenergies in Table I turn out to be almost independent of the choice of the additional boundary condition. Vanishing excitonic polarization as well as vanishing spatial derivative of the excitonic polarization at the surface are used, either with the longitudinal exciton branch being excited, or alternatively this branch not being excited. These conditions indeed reveal different behavior of the excitons, but the eigenenergies obtained from fits to ATR spectra lie always at considerably higher energies than those obtained from fits to reflection spectra. This finding appears to be systematic. An explanation will be given in Secs. IV and V.

IV. PENETRATION DEPTH OF LIGHT

In this section let me consider a crystal having for simplicity only *one* single excitonic resonance showing spatial dispersion. Then, the wave-vector-dependent dielectric function is given by[2]

$$\epsilon(\omega,k)=\epsilon_\infty\left(1+\frac{\omega_L^2-\omega_T^2}{\omega_T^2-\omega^2+\beta k^2-i\omega\Gamma}\right) . \quad (4)$$

This function and the dispersion equation for bulk polaritons[30]

$$c^2k^2/\omega^2=\epsilon(\omega,k) \quad (5)$$

yield the frequency versus wave-vector dispersion relation for excitonic polaritons as shown schematically in Fig. 3 (c is the vacuum velocity of light). This dispersion relation consists of the lower and the upper polariton branch denoted with 1 and 2, respectively.[2]

The normal-incidence-reflection spectrum of a crystal with optical properties described by Eqs. (4) and (5) is shown in the upper part of Fig. 4. The parameters are chosen for the $C_{n=1}$ exciton in ZnO, however, with the excitonic polarization assumed to be isotropic (see Table I). The damping is chosen to be $\hbar\Gamma=0.7$ meV, the thickness of an exciton-free surface layer $d_0=0$.

Let me make an assumption for the following calculation. I assume for a moment that only one polariton branch is excited in the crystal, either the lower or the upper polariton branch. Then, I ask for the reflection spectrum of such a crystal in which only one polariton branch is excited. The result is shown in the middle part of Fig. 4 for the lower branch (denoted with 1) and the upper branch (2). From a comparison of the upper and the middle part of Fig. 4 one can see that the pronounced structure in normal-incidence-reflection spectra is due to the lower polariton branch at energies around the transverse eigenenergy (C_T) and is due to the upper polariton branch at energies around the longitudinal eigenenergy of the exciton (C_L).

Next, I return to the model crystal in which *all* po-

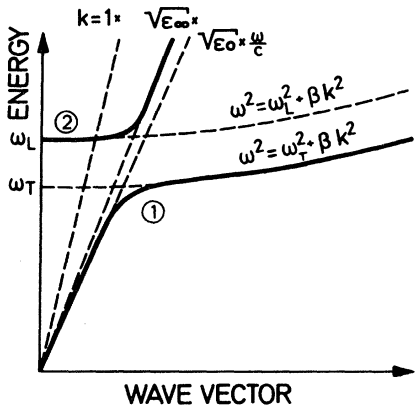

FIG. 3. Schematic energy vs wave-vector dispersion relation for excitonic polaritons with spatial dispersion.

lariton branches are excited simultaneously. I ask for the penetration depth of the light impinging on the crystal surface to get an impression from which parts of the crystal the reflection spectrum is determined. The lower part of Fig. 4 shows the penetration depth from the crystal surface in which the electric field amplitude of each branch decreases to $1/e$. This depth is calculated using the complex dielectric function or refractive index for each of both branches.[2] All three diagrams of Fig. 4 together show that the pronounced structure of normal-incidence-reflection spectra of excitonic polaritons reveal crystal properties from regions up to approximately 100 nm for the parameters chosen in Fig. 4.

The analogous calculations done for an attenuated-total-reflection experiment are presented in Fig. 5. In this geometry, the longitudinal branch is included (denoted with L). The damping is chosen to be $\hbar\Gamma = 2$ meV. It is seen that the ATR spectrum is determined mainly by the upper polariton branch (denoted with 2) whose dielectric function is negative between the transverse and longitudinal resonance frequencies. The penetration depth of this branch is clearly less than 50 nm in the energy region of interest because the polariton wave of this branch is nearly evanescent.[13]

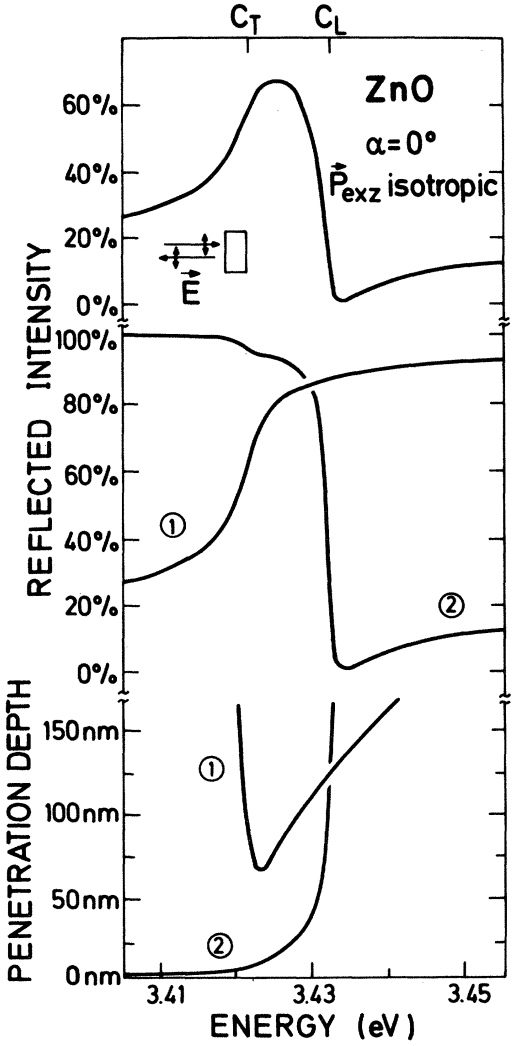

FIG. 4. Normal-incidence-reflection spectrum calculated for a material with assumed iostropic exciton polarization (upper part) and calculated for a fictitious material with only the lower (1) or the upper polariton branch (2) being excited (middle part). Penetration depth of light for a material with both branches being excited (lower part).

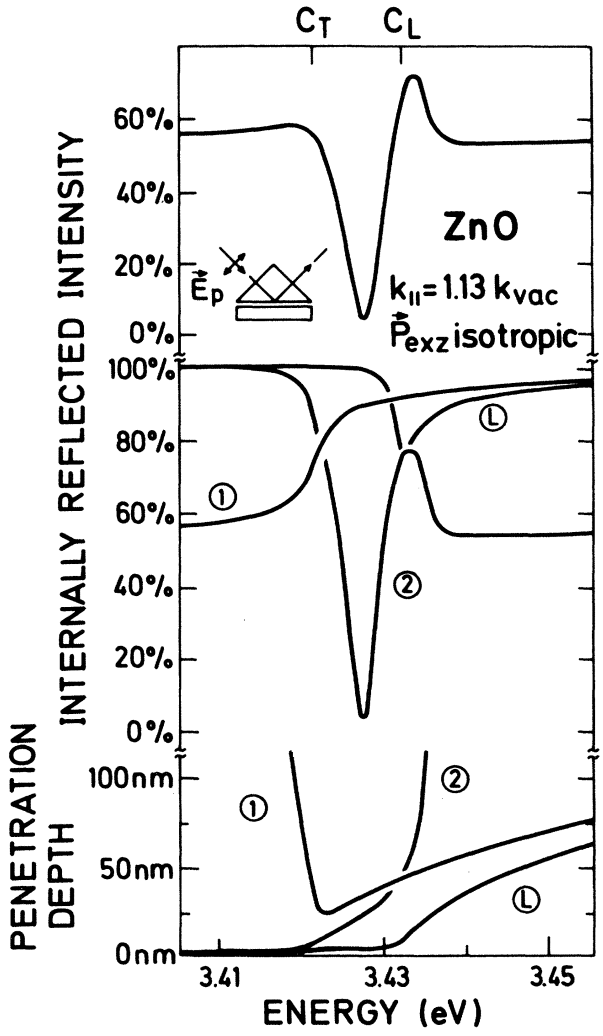

FIG. 5. Attenuated-total-reflection spectrum calculated for a material with assumed isotropic exciton polarization (upper part) and calculated for a material with only the lower (1), the upper (2), or the longitudinal branch (L) being excited (middle part). Penetration depth of light for a material with all three branches being excited (lower part).

As a consequence, the deviations of the parameters in Table I obtained so far for reflection and ATR can be explained by the different penetration depths of excitonic polaritons. An ATR experiment probes spatial regions close to the crystal surface, whereas a reflection experiment probes deeper into the crystal bulk.

Thus, the results of Figs. 1 and 2 yield an increased damping of excitonic polaritons close to the crystal surface, and above all, a considerable increase of excitonic eigenenergies in near-surface crystal regions.

V. EXPLANATION OF EXPERIMENTAL SPECTRA WITH DEPTH-DEPENDENT EXCITONIC EIGENENERGIES AND DAMPING

The reason for the experimentally observed depth dependence of excitonic eigenenergies can be found in the bending of the energy bands near to the crystal surface. Such a band bending is always present at real semiconductor surfaces. As a consequence, an exciton feels an increasing electric field when approaching the crystal surface from the crystal bulk.

Some years ago, Blossey has calculated the behavior of an exciton in an electric field.[31] At weak electric fields the excitonic eigenenergy $\hbar\omega_{Exz}$ undergoes a Stark shift to lower energies. With increasing field strength the eigenenergy shifts to higher energies because the Coulomb well of the exciton, which is an electron-hole pair bound together by Coulomb attraction, is lowered by the energy of the electric field. Simultaneously, the damping of the exciton increases with increasing electric field strength. The result of Blossey's theory is shown in Fig. 6 (after Ref. 31). The electric field strength E is plotted in units of the ionization field strength E_I of the exciton. At this field strength E_I the product of the electric field strength and the excitonic Bohr radius equals the excitonic binding or Rydberg energy R_{Exz}. The electric field dependence of the excitonic eigenenergy and the depth dependence of the electric field lead to a depth dependence of the eigenenergy and damping in case of band bending at the crystal surface.

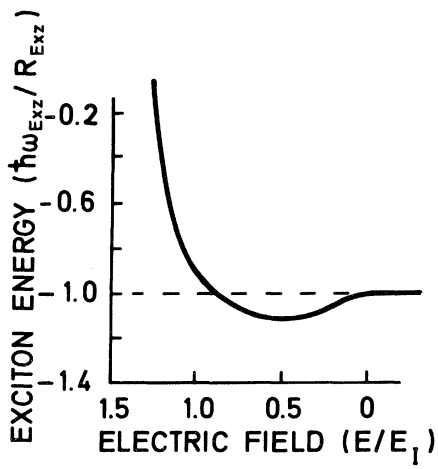

FIG. 6. Eigenenergy of excitons in an electric field (after Ref. 31).

This spatial behavior of the excitonic eigenenergies and damping should be included in model calculations for reflection and attenuated-total-reflection spectra. Skaistis and Sugakov,[18] Sakoda,[20] and especially Kiselev[22] showed normal-incidence-reflection spectra calculated with a variety of different depth dependences of excitonic eigenenergies. However, they made no attempt to compare their results with experimental spectra to extract information about the behavior of excitons nor did they apply the model to attenuated total reflection.

As a first step, I approximate the continuous depth dependence by a four-layer model consisting of an exciton-free surface layer (thickness d_0), of three layers with modified excitonic eigenenergies and damping (each of them with thickness d), and of the crystal bulk. The three layers contain excitons with spatial dispersion. Continuity of the vector of excitonic polarization is chosen as the additional boundary condition between the exciton-free surface layer and the uppermost layer containing excitons[2,7]; continuity of the vector of excitonic polarization and its normal derivative are chosen as the conditions at all other inner boundaries.[22] Such a model leads to a system of linear equations which has to be solved numerically. The number of equations increases, for instance, from 17 in case of normal-incidence reflection of a crystal with one excitonic resonance described by Eq. (4) to 40 in case of attenuated total reflection of a crystal with two excitonic resonances described by Eq. (1).

The depth dependence used for the eigenenergies of the $B_{n=1}$ exciton in ZnO is shown in Fig. 7. The energies decrease from a bulk value (called ω_{TV} and ω_{LV} in Table I) to lower energies ($\omega_{TV}+\Delta\omega_3$, $\omega_{LV}+\Delta\omega_3$; $\omega_{TV}+\Delta\omega_2$, $\omega_{LV}+\Delta\omega_2$) and then increase near to the crystal surface ($\omega_{TV}+\Delta\omega_1$, $\omega_{LV}+\Delta\omega_1$). Simultaneously, the damping constant increases linearly from the bulk value Γ_V to a value of $\Gamma_V+\Delta\Gamma$ in the uppermost layer containing excitons.

The results obtained from fits with this model are shown in Fig. 8. The experimental spectra are the same spectra as in Figs. 1 and 2. An experimental normal-incidence-reflection spectrum (weak line) is compared in the upper part with a theoretical one (strong line) calculated with the depth-dependent behavior of excitonic polaritons. The parameters obtained from the fit are given in Table I. It should be mentioned, that the actual value of the parameters is not determined uniquely because they are not completely independent from each other as mentioned

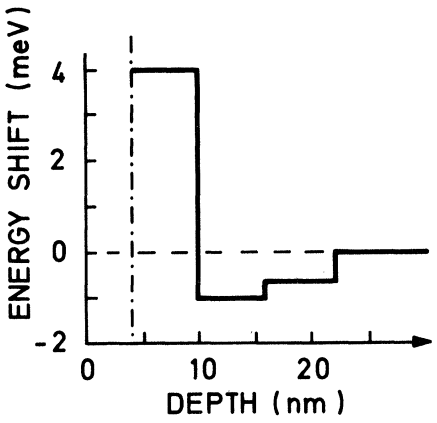

FIG. 7. Depth dependence of excitonic eigenenergies of the $B_{n=1}$ exciton in ZnO as used for calculating reflection and ATR spectra.

also in Ref. 22. Therefore, it is difficult at the moment to derive predictions about the exact shape of the band bending at the surface. The model calculation leads to an excellent agreement with the experiment, especially also in the energy region around B_L, the longitudinal eigenenergy of the B exciton. The identical set of parameters as obtained from fit to normal-incidence reflection is used to calculate the attenuated-total-reflection spectrum shown in the lower part of Fig. 8 (strong line). This theoretical spectrum also fits the experimental one (weak line) very well.

The excellent agreement between the experiments for different geometries and the calculations gives strong support for a spatial dependence of the excitonic eigenenergies and damping near the crystal surface.

The fits can be improved even more by varying the damping independently for fits to experimental reflection and ATR spectra. It turns out that the damping for ATR spectra is higher than those for reflection spectra as already seen in Figs. 1 and 2. This finding may be due to an additional damping by surface irregularities which act primarily on *surface* polaritons excited in an ATR experiment.[13] Such additional damping is not included in the calculations but can be simulated by increasing the damping constant for the attenuated-total-reflection arrangement.

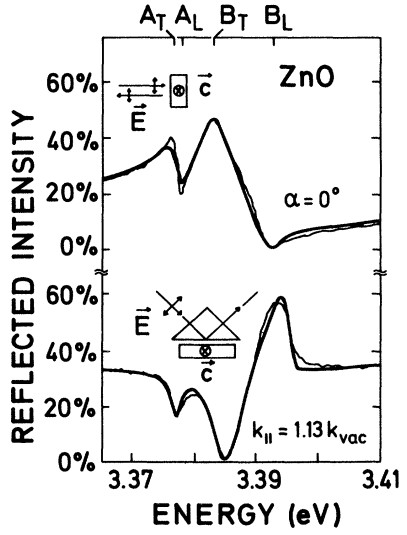

FIG. 8. Normal-incidence-reflection (upper part) and attenuated-total-reflection spectra (lower part) of the $A_{n=1}$ and $B_{n=1}$ excitonic polaritons in ZnO. The experimental spectra (weak lines) are the same as in Figs. 1 and 2. The theoretical spectra (strong lines) are calculated with one homogeneous set of parameters for reflection and ATR including a depth dependence of the excitonic eigenenergies and damping.

VI. NORMAL-INCIDENCE REFLECTION OF VARIOUS SEMICONDUCTORS

In this section, I want to demonstrate that the findings reported above describe a basic property of excitonic polaritons in semiconductors. Searching through the literature it is very difficult to find truly quantitatively good fits even to the simplest case of normal-incidence-reflection spectra of crystals with excitonic polaritons.

Let me consider materials which show one single

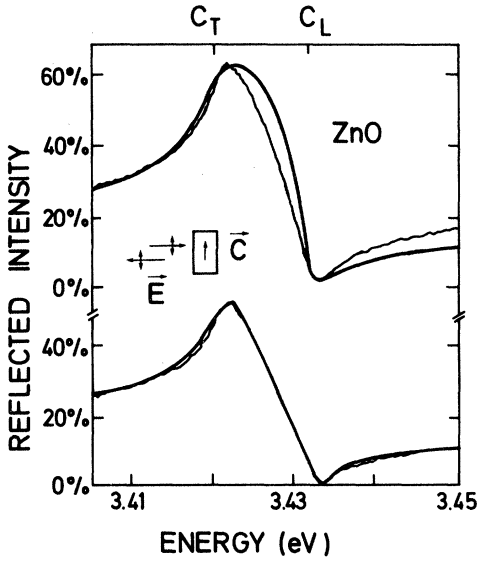

FIG. 9. Normal-incidence-reflection spectra of the $C_{n=1}$ excitonic polaritons in ZnO. The experimental spectra (weak lines) are identical in upper and lower part. Theory (strong lines) with constant (upper part) and depth-dependent eigenenergies and damping (lower part).

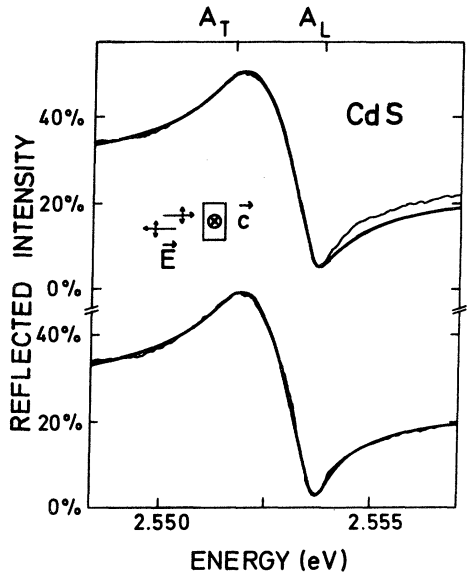

FIG. 10. Normal-incidence-reflection spectra of excitonic polaritons in CdS. The experimental spectra (weak lines) are identical in upper and lower part. Theory (strong lines) with constant (upper part) and depth-dependent eigenenergies and damping (lower part).

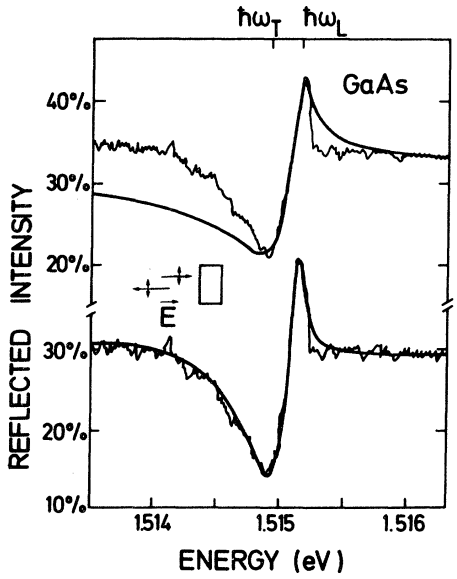

FIG. 12. Normal-incidence-reflection spectra of excitonic polaritons in GaAs. The experimental spectra (weak lines) are identical in upper and lower part. Theory (strong lines) with constant (upper part) and depth-dependent eigenenergies and damping (lower part).

excitonic transition: ZnO and CdS for light polarized parallel to the hexagonal $\vec{c}$ axis, or cubic ZnSe and GaAs. These materials reveal very different properties of excitons in semiconductors and are chosen therefore as model materials. Fits are obtained in the literature so far with calculations including an exciton-free surface layer and a crystal bulk with excitons showing spatial dispersion, but not showing depth-dependent eigenenergies. The standard of such best fits is shown in the upper parts of Figs. 9–12 for ZnO, CdS, ZnSe, and GaAs. The parame ters are given in Table I. The description of the experimental spectra fails considerably in some energy region for all four semiconductors.

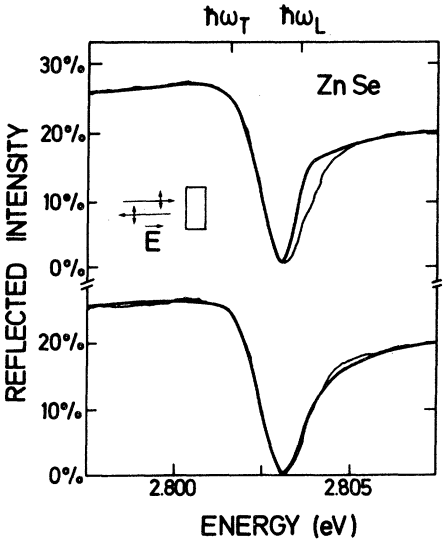

FIG. 11. Normal-incidence-reflection spectra of excitonic polaritons in ZnSe. The experimental spectra (weak lines) are identical in upper and lower part. Theory (strong lines) with constant (upper part) and depth-dependent eigenenergies and damping (lower part).

A slight improvement of the description might be obtained by considering a depth-dependent damping of excitons. However, the calculations done with such a dependence have omitted spatial dispersion of excitons.[8,32]

The depth dependence of eigenenergies and damping of excitonic polaritons with spatial dispersion is included in the lower parts of Figs. 9–12. They exhibit the same experimental spectra as the upper parts (weak lines) compared with theoretical ones calculated with the model described above. Now, the agreement is really excellent in the whole energy region of the excitons for all different semiconductors.

This agreement confirms the statement that excitonic polaritons show a depth-dependent behavior of their properties in regions near the crystal surface. This behavior seems to be a fundamental property of excitons in semiconductors.

VII. CONCLUSIONS

The experiments and the calculations described in this paper show that the properties of excitonic polar-

itons vary with the exciton's distance from the crystal surface. An experimental normal-incidence-reflection spectrum therefore always reveals a strong influence of such a transition region near to the surface, and this influence determines the reflection structure in addition to the properties given by the dielectric function in the crystal bulk. As a consequence, one has to be very cautious in deriving statements about the bulk properties of excitonic polaritons from reflection experiments without considering this transition region. Reflection spectra do not reveal pure bulk properties of excitons.

A long-lasting discussion in the literature is the discussion about the additional boundary conditions for excitonic polaritons.[4] There have been several attempts to make a decision about the appropriate boundary condition from fitting reflection spectra. Such decisions seem to be at least questionable in view of the results of this paper and have to be reconsidered. The influence of the additional boundary conditions on reflection spectra of excitons is much less than the influence of the modified excitonic eigenenergies and damping at the crystal surface!

In conclusion, this paper reported the result of experiments which manifested the modified properties of excitons near a semiconductor surface. This modification is verified by measurements and model calculations of normal-incidence-reflection and attenuated-total-reflection spectra of excitonic $n = 1$ transitions in various semiconductors. It is desirable that these results will stimulate more detailed calculations of microscopic models, for example the consideration of a continuous-transition region.

ACKNOWLEDGMENTS

I thank E. Bauser, R. Helbig, and the Kristall- und Materiallabor der Universität Karlsruhe for supplying the samples used in this investigation. I am also grateful to H. J. Queisser, B. Fischer, A. A. Maradudin, F. Stern, and R. Zeyher for many helpful discussions, and to H. G. Fischer and W. Heinz for technical assistance. I was supported by the Deutsche Forschungsgemeinschaft.

[1]J. J. Hopfield, Phys. Rev. 112, 1555 (1958).
[2]J. J. Hopfield and D. G. Thomas, Phys. Rev. 132, 563 (1963).
[3]S. I. Pekar, Zh. Eksp. Teor. Fiz. 33, 1022 (1957) [Sov. Phys. JETP 6, 785 (1958)]; J. Phys. Chem. Solids 5, 11 (1958).
[4]See, for instance: R. Zeyher, J. L. Birman, and W. Brenig, Phys. Rev. B 6, 4613 (1972); A. A. Maradudin and D. L. Mills, *ibid.* 7, 2787 (1973); M. J. Frankel and J. L. Birman, *ibid.* 13, 2587 (1976); D. L. Johnson and P. R. Rimbey, *ibid.* 14, 2398 (1976); F. García-Moliner and F. Flores, J. Phys. (Paris) 38, 851 (1977); A. Stahl, Phys. Status Solidi (B) 92, 113 (1979); F. Forstmann, Z. Phys. 32, 385 (1979); A. D'Andrea and R. Del Sole, Solid State Commun. 30, 145 (1979); A. A. Demidenko, S. I. Pekar, and E. Tsekvava, Zh. Eskp. Teor. Fiz. 76, 1445 (1979) [Sov. Phys. JETP 49, 735 (1979)]; R. Zeyher, in *Proceedings of the 1980 Annual Conference Condensed Matter Division of the European Physical Society, Antwerpen,* edited by J. T. Devreese (Plenum, New York, 1981).
[5]See, for instance: K. Germanova, K. Marinova, and S. Stoyanov, Phys. Status Solidi (B) 88, K19 (1978); I. Broser and M. Rosenzweig, *ibid.* 95, 141 (1979); W. Stössel and H. J. Wagner, *ibid.* 96, 369 (1979); W. Dreybrodt, K. Cho, S. Suga, F. Willmann, and Y. Niji, Phys. Rev. B 21, 4692 (1980), and references therein.
[6]K. Hümmer and P. Gebhardt, Phys. Status Solidi (B) 85, 271 (1978).
[7]J. Lagois, Phys. Rev. B 16, 1699 (1977).
[8]J. Lagois, E. Wagner, W. Bludau, and K. Lösch, Phys. Rev. B 18, 4325 (1978).
[9]See, for instance: V. A. Kiselev, B. S. Razbirin, and I. N. Uraltsev, Phys. Status Solidi (B) 72, 161 (1975); M. DeCrescenzi, G. Harbeke, and E. Tosatti, Solid State Commun. 32, 777 (1979); B. Dietrich and J. Voigt, Phys. Status Solidi (B) 93, 669 (1979), and references therein.
[10]See, for instance: R. G. Ulbrich and C. Weisbuch, Phys. Rev. Lett. 38, 865 (1977); N. Allen and E. O. Kane, Solid State Commun. 28, 965 (1978); E. S. Koteles and G. Winterling, Phys. Rev. Lett. 44, 948 (1980); C. Hermann and P. Y. Yu, Phys. Rev. B 21, 3675 (1980); P. Y. Yu, in *Topics in Current Physics,* edited by K. Cho (Springer, Heidelberg, 1979) Vol. 14, p. 211, and references therein.
[11]J. Lagois and B. Fischer, Phys. Rev. Lett. 36, 680 (1976).
[12]I. Hirabayashi, T. Koda, Y. Tokura, J. Murata, and Y. Kaneko, J. Phys. Soc. Jpn. 40, 1215 (1976).
[13]B. Fischer and J. Lagois, in *Topics in Current Physics,* edited by K. Cho (Springer, Heidelberg, 1979), Vol. 14, p. 183, and references therein.
[14]J. Lagois and B. Fischer, in *Surface Polaritons—Modern Problems in Solid State Physics,* edited by D. L. Mills and V. M. Agranovich (North-Holland, Amsterdam, 1981).
[15]M. F. Deigen and M. D. Glinchuk, Fiz. Tverd. Tela (Leningrad) 5, 3250 (1963) [Sov. Phys. Solid State 5, 2377 (1964)].
[16]M. S. Brodin, A. V. Kritsky, E. N. Myasnikov, M. I. Strashnikova, and L. A. Shlyakhova, Ukr. Fiz. Zh. (Russ. Ed) 18, 828 (1973).
[17]N. A. Davydova, E. N. Myasnikov, and M. I. Strashnikova, Fiz. Tverd. Tela (Leningrad) 16, 1173 (1974) [Sov. Phys. Solid State 16, 752 (1974)].
[18]E. Skaistis and V. I. Sugakov, Liet. Fiz. Rinkinys 14, 297 (1974).
[19]V. I. Sugakov and V. N. Khotyaintsev, Zh. Eksp. Teor. Fiz. 70, 1566 (1976) [Sov. Phys. JETP 43, 817 (1976)].
[20]S. Sakoda, J. Phys. Soc. Jpn. 40, 152 (1976).
[21]I. Balslev, Phys. Status Solidi (B) 88, 155 (1978).
[22]V. A. Kiselev, Fiz. Tverd. Tela (Leningrad) 20, 2173 (1978) [Sov. Phys. Solid State 20, 1255 (1978)]; 21, 1069 (1979) [21, 621 (1979)]; Pis'ma Zh. Eksp. Teor. Fiz. 29, 369 (1979) [JETP Lett. 29, 333 (1979)].
[23]R. Helbig, J. Cryst. Growth 15, 25 (1972).

[24]D. G. Thomas, J. Phys. Chem. Solids 15, 86 (1960).
[25]E. Grobe and H. Salow, Z. Angew. Phys. 32, 381 (1972).
[26]CODATA Bull. 11, 7 (1973).
[27]H. S. Stewart and R. F. Hopfield, in *Applied Optics and Optical Engineering,* edited by R. Kingslake (Academic, New York, 1965), Vol. I, p. 127.
[28]See, for instance: A. Otto, in *Festkörperprobleme—Advances in Solid State Physics,* edited by H. J. Queisser (Vieweg, Braunschweig, 1974), Vol. XIV, p. 1.
[29]The details of calculation are given in Ref. 7; J. Lagois and B. Fischer, Solid State Commun. 18, 1519 (1976).
[30]K. Huang, Proc. R. Soc. London Ser. A 208, 352 (1951).
[31]D. F. Blossey, Phys. Rev. B 3, 1382 (1971).
[32]W. Ekardt, K. Lösch, and D. Bimberg, Phys. Rev. B 20, 3303 (1979).